A Quiet Helicopter for Air Taxi Operations

Wayne Johnson
NASA Ames Research Center
Moffett Field, California
wayne.johnson@nasa.gov

ABSTRACT

NASA is exploring rotorcraft designs for VTOL air taxi operations, also known as urban air mobility (UAM) or on-demand mobility (ODM) applications. Several concept vehicles have been developed, intended to focus and guide NASA research activities in support of aircraft development for this emerging market. This paper examines a single main-rotor helicopter designed specifically for low-noise air taxi operations. Based on demonstrated technology, the aircraft uses a turboshaft engine with a sound-absorbing installation, and the NOTAR anti-torque system to eliminate tail-rotor noise, consequently the noise and annoyance of the aircraft are dominated by the main rotor. Several design parameters are explored to reduce the noise, including rotor tip speed, blade geometry, and higher-harmonic control. Commensurate with the level of design detail, the noise is calculated for compact loading and thickness sources on the rotating blades. The metric is the reduction of the noise for the helicopter certification conditions (takeoff, flyover, and approach), relative a baseline aircraft with typical (high) tip speed, conventional blade planform, and no higher-harmonic control.

INTRODUCTION·

Urban air taxi operations, also known as urban air mobility (UAM) or on-demand mobility (ODM) applications, are enabled by vertical take-off and landing (VTOL) capability. The power and energy requirements of VTOL aircraft are minimized by using low disk-loading rotors, and requiring only short range permits consideration of non-traditional propulsion concepts. The community of innovation has recognized that technology advances in structures, automation and control, energy generation-storage-utilization, and tools for design and analysis, coupled with pressures of resource availability and population density, make this the right time to explore new ways to move people and goods.

The NASA Revolutionary Vertical Lift Technology project (RVLT) has been developing tools and datasets to support the design of advanced vertical lift aircraft. In the last few years, this work has focused on the development of multidisciplinary tools for design and optimization of aircraft with low emissions and low acoustics as objectives. These tools and processes are now also being applied to the new design challenges brought by UAM requirements.

The NASA RVLT project is developing UAM rotorcraft designs (Refs. 1–4) that can be used to focus and guide research activities in support of aircraft development for emerging aviation markets. These NASA concept vehicles encompass relevant technologies (including battery, hybrid, internal-combustion propulsion, distributed electric propulsion, highly efficient yet quiet rotors), although and are different in appearance and design detail from prominent industry arrangements. The design work also provides a context for developing design and analysis tools. The concept vehicles developed include quadrotor, side-by-side helicopter, and lift+cruise configurations (Ref. 4), illustrated in Figure 1. Additional concept vehicles are currently being examined, including a tiltwing aircraft and a ducted-fan configuration.

Generally absent from consideration for UAM applications is the single main-rotor helicopter, in spite of its important benefit of a known path for certification. This paper examines a single main-rotor helicopter designed specifically for low-noise air taxi operations (Fig. 2). Based on demonstrated technology, the aircraft uses a turboshaft engine with a sound-absorbing installation, and the NOTAR (NO TAil Rotor) anti-torque system to eliminate tail-rotor noise, consequently the noise and annoyance of the aircraft are dominated by the main rotor. Several design parameters are explored to reduce the noise, including rotor tip speed, blade geometry, and higher-harmonic control.

Quadrotor
turboshaft or battery

Side-by-Side Helicopter
turboshaft or battery

Lift+Cruise VTOL
turbo-electric or battery

Figure 1. Air taxi aircraft designs: six occupants (1200 lb payload), 75 nm range.
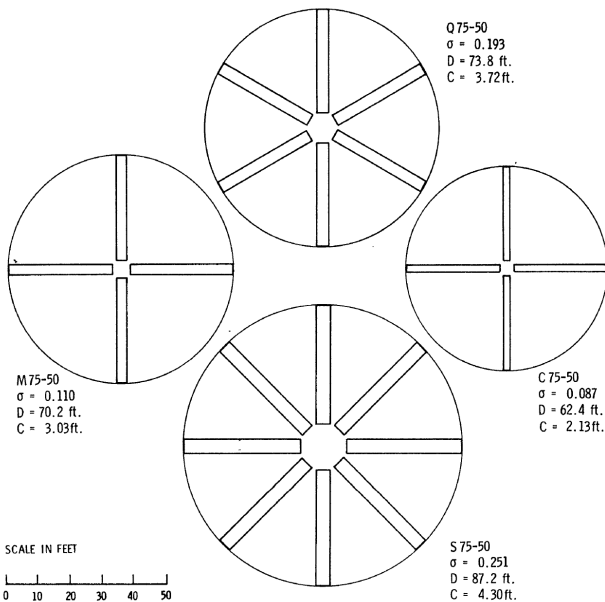

Figure 2. Quiet Single-Main Rotor Helicopter.

Q 75-50
σ = 0.193
D = 73.8 ft.
C = 3.72 ft.

M 75-50
σ = 0.110
D = 70.2 ft.
C = 3.03 ft.

C 75-50
σ = 0.087
D = 62.4 ft.
C = 2.13 ft.

S 75-50
σ = 0.251
D = 87.2 ft.
C = 4.30 ft.

SCALE IN FEET

0   10   20   30   40   50

Figure 3. Rotor designs for tradeoff between noise and cost (Ref. 16).
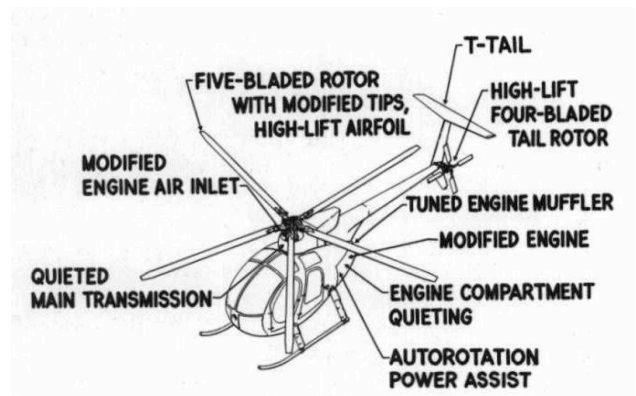
Figure 4. OH-6A quiet helicopter (Ref. 9).

2

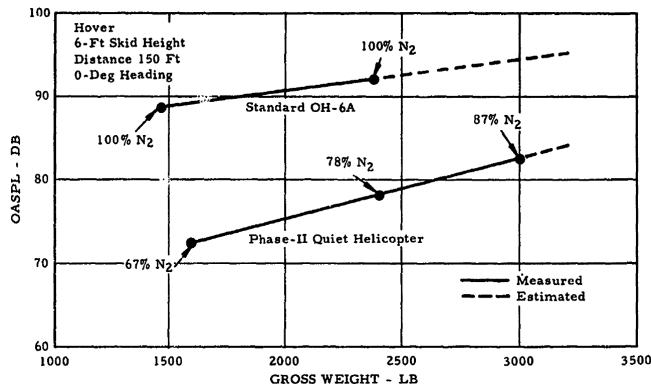Figure 5. OH-6A noise level comparison in hover (Ref. 10).

Figure 6. Blue Edge^{TM} planform of H160-B main rotor (Ref. 33).

QUIET HELICOPTER RESEARCH

The impact of rotor noise on community acceptance of helicopters was recognized early, so there has been five decades of work on reducing noise (Refs. 5-33). From the beginning, much of the focus was on the design variables of tip speed and tail rotor size (Refs. 5, 6, 9).

Faulkner (Refs. 6, 16) examined the tradeoff between helicopter noise and direct operating cost (DOC), for 50-passenger tandem helicopters operated over a range of 400 nm. The rotorcraft were designed for minimum DOC at a given noise goal, with the noise goal met using low tip speed and high solidity rotors. Noise was estimated using the empirical noise formula of Reference 34. Four advanced technology designs were developed: unconstrained, moderately quiet, very quiet, and extremely quiet, for which the tip speed ranged from 680 to 270 ft/sec, the number of blades from 4 to 8, and the solidity ratio from 0.11 to 0.25 (Figure 3). Relative the unconstrained design, the moderately/very/extremely quiet designs achieved 8/14/19 dB reduction of OASPL, for a 9/26/56% increase in DOC.

The Quiet Helicopter Program of the Advanced Research Projects Agency (ARPA) explored reduction of noise signatures of Sikorsky SH-3A, Kaman HH-43B, and Hughes OH-6A helicopters (Refs. 8-15). All of these aircraft (baseline and modified) were tested by NASA (Refs. 8, 13, 15). The OH-6A helicopter had the most extensive modifications, achieving the best results (Refs. 9-13). The quiet OH-6A (Figure 4) had a low tip speed of the main rotor (reduced from 646 to 433 ft/sec, 67%) and lower gross weight (reduced from 2100 to 1600 lb). A blade was added to the main rotor (5 blades on the modified aircraft), increasing the solidity from 0.054 to 0.068, and the modified blade had a drooped and tapered tip. The tail radius was increased, and the number of blades doubled, for a 30% increase in tail rotor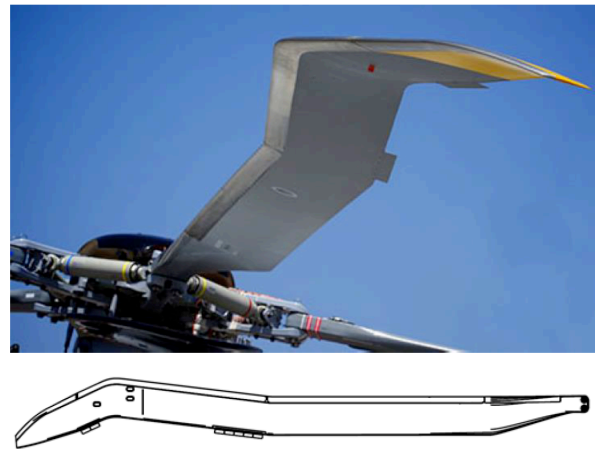 area, and a factor 2.28 increase in total blade area. The engine noise was suppressed. The noise of the modified OH-6A was reduced by 14-16 dB OASPL in level flight, 17-20 dB OASPL in hover, operating at 67% rpm and 1600 lb gross weight; and reduced by 14 dB in hover for 78% rpm, 2400 lb (Figure 5, Refs. 10, 13).

The Blue Edge rotor development for the H160-B helicopter by Airbus Helicopters (Refs. 30-33) is a recent example of successfully minimizing helicopter noise through design choices. An advanced main rotor planform reduces the blade-vortex interaction noise (Figure 6), the rotor rotational speed is automatically changed during operations close to ground and populated areas, and a low-noise, canted ducted tail-rotor is used. This aircraft achieves a noise certification level in approach that is 7 dB below the ICAO limit (Ref. 33).

QUIET HELICOPTER CONFIGURATION

The quiet single-main rotor helicopter (QSMR) configuration is illustrated in Figure 2. As for the other concept vehicles, the QSMR is designed for six occupants (1200 lb payload) and a range of 75 nm (further details of the design mission are given below). The propulsion system uses two turboshaft engines. To avoid tail rotor noise, the NOTAR (NO TAil Rotor) anti-torque system is used. For this aircraft, the optimum disk loading (resulting in minimum gross weight for the mission) is 4.0 lb/ft2. To reduce the noise from the main rotor, a low tip speed will be used, which will require a large blade area and a large number of blades. The direct and indirect results of low tip speed include high rotor and transmission weight, which will increase the aircraft takeoff weight. Consequently, there will be a limit on the noise reduction achievable by reducing the tip speed. Further reductions in noise require consideration of other design parameters, including blade shape and higher-harmonic control.

3

DESIGN AND ANALYSIS TOOLS

The aircraft were sized and optimized using NDARC. The rotorcraft comprehensive analysis CAMRAD II was used to optimize the rotor performance, and to calculate blade airloads for the noise analysis. The aircraft sound was calculated considering loading, thickness, and broadband noise sources.

Rotorcraft Sizing and Analysis NDARC

The concept vehicles were sized using NDARC (NASA Design and Analysis of Rotorcraft), which is a conceptual/preliminary design and analysis code for rapidly sizing and conducting performance analysis of new aircraft concepts (Ref. 35). NDARC has a modular architecture, facilitating its extension to new aircraft and propulsion types, including non-traditional propulsion systems. The design task sizes the vehicle to satisfy a set of design conditions and missions. The aircraft size is characterized by parameters such as design gross weight, weight empty, component dimensions, drive system torque limit, fuel tank capacity, and engine power. The analysis tasks include off-design mission analysis and flight performance calculation for point operating conditions. To achieve flexibility in configuration modeling, NDARC constructs a vehicle from a set of components, including fuselage, rotors, wings, tails, transmissions, and engines. For efficient program execution, each component uses surrogate models for performance and weight estimation. Higher fidelity component design and analysis tools as well as databases of existing components provide the information needed to calibrate these surrogate models, including the influence of size and technology level. The reliability of the synthesis and evaluation results depends on the accuracy of the calibrated component models.

Comprehensive Analysis CAMRAD II

Performance analyses were conducted with the comprehensive rotorcraft analysis CAMRAD II (Refs. 36–37). CAMRAD II is an aeromechanics analysis of rotorcraft that incorporates a combination of advanced technologies, including multibody dynamics, nonlinear finite elements, and rotorcraft aerodynamics. The trim task finds the equilibrium solution for a steady state operating condition, and produces the solution for performance, loads, and vibration. The CAMRAD II aerodynamic model for the rotor blade is based on lifting-line theory, using steady two-dimensional airfoil characteristics and a vortex wake model. CAMRAD II has undergone extensive correlation with performance and loads measurements on rotorcraft.

In order to resolve the fast variation of blade airloads during interaction with the rotor tip vortices, a small azimuth time step is required, 1.5 deg for the present work. CAMRAD II solves for the coupled aerodynamic loading, rigid and elastic blade motion, and aircraft trim using a time step of 12 to 15 deg. Then the blade motion and trim are frozen, and the aerodynamics (wake and airloads) are evaluated for the smaller time step. The use of CAMRAD II in calculation of rotorcraft noise is described in Ref. 38. To obtain realistic blade-vortex interaction airloads using lifting-line theory and a small azimuthal step size, a large vortex core radius (here 80% chord) is used, as recommended by Boyd (Ref. 38).

Acoustic Analysis

The calculation of the rotor loading and thickness noise is based on the Ffowcs Williams and Hawkings equations, Farassat 1A formulation (Refs. 39–41). The aerodynamic model of CAMRAD II does not produce the loading on the surface of the blade, instead the interface between the wing solution and wake solution (and with the beam elements in the structural model) is in terms of section loading: lift, drag, and moment at radial stations along the high aspect-ratio blade. For highest fidelity, computational fluid dynamics (perhaps coupled with CAMRAD II for the blade motion and trim) calculations of the near field provide input for the acoustic integral formulations to calculate the radiated noise. For the present work, commensurate with the level of design detail available in the present investigation, the noise is calculated for compact loading and thickness sources on the rotating blades, the blade airloads and motion obtained from CAMRAD II output. This noise calculation does not include the effects of atmospheric attenuation or ground reflection.

Broadband noise of the helicopter rotor is calculated using the model of Pegg (Ref. 42) or Brooks (Refs. 43–44), which gives the spectrum as a function of tip speed, thrust, blade area, and mean lift coefficient.

The overall sound pressure level (OASPL) is obtained from the total mean-square pressure. Since the subjective perception of sound depends on the frequency content, a number of frequency-weighted measures of the sound pressure level have been developed. The perceived noise level (PNL) is a metric developed for aircraft, using a weighting that depends on both the magnitude and the frequency of the spectrum, based on the sound annoyance level. Further corrections have been developed for aircraft noise. The effective perceived noise level (EPNL) accounts for the sound duration and the presence of discrete frequency tones. PNL and EPNL are defined in FAR Part 36 (Ref. 45).

The noise certification requirements are specified in FAR Part 36, Appendix H, "Noise Requirements for Helicopters" (Ref. 45). The aircraft is flown over three microphones, at the centerline and 150 m to starboard and port. The operating conditions are sea level pressure, and a temperature of 25°C. Three trajectories are flown: takeoff, flyover, and approach. The takeoff profile starts 500 m from the center microphone, 20 m above ground level, and is flown at best rate of climb, V_y (best rate of climb speed) and 100% maximum rated

power. The flyover profile is 150 m above ground level, for this aircraft flown at $0.9V_H$, where V_H is the speed at 100% maximum continuous power. The approach profile has a 6-degree descent angle, flown at V_y, 120 m above ground level at the center microphone. Certification requirements specify the maximum EPNL for these trajectories. NDARC was used to calculate V_y, V_H, and the takeoff climb angle.

This investigation uses the certification metric to assess the impact of design parameters on the helicopter noise. With the assumption of compact loading in the noise calculation, a comparison with the certification requirement is not appropriate, rather the noise is compared with that of a baseline aircraft with typical (high) tip speed, conventional blade planform, and no higher-harmonic control.

UAM DESIGN MISSION

Following an initial air taxi vehicle study, which explored vehicle technology themes using aircraft of various sizes designed for several candidate missions, RVLT performed a focused study to better understand a particular urban air mobility market. A design mission was developed accounting for the existing geography, population patterns, infrastructure, and weather in twenty-eight markets across the United States of America (Ref. 3). The resulting mission is to carry six passengers (including the pilot, if not autonomous; 1200 lb) on two 37.5-nm flights (total 75-nm range without recharging or refueling), with a 20 min reserve (Figure 7). Takeoff altitude is 6000-ft (ISA), and cruise is at best range speed, 4000-ft above ground level. This mission is intended to be used as a sizing requirement. The actual operational missions flown by the aircraft will be different, driven by economics, air traffic, and other aspects of a particular flight.

TECHNOLOGY

Technology assumptions were made to size the quiet helicopter, consistent with the assumption used to develop the other concept vehicles:
a) Structures (TRL 3+): composite VTOL structures, lightweight tail boom.
b) Aerodynamics (TRL 5+): passive rotor and airframe lift/drag.

c) Propulsion (TRL 5+): high torque-to-weight transmissions.
d) Systems (TRL 5+): equipment for instrument flight rules (IFR) operations (hence autonomy possible without additional weight); environmental control systems, insulation, seating.

Weights

The design gross weight is the mission takeoff weight. The structural design gross weight is taken as the design gross weight, with an ultimate load factor of 4. The maximum takeoff weight is calculated for hover out-of-ground-effect, at 100% MRP.

NDARC parametric weight models (Ref. 35) are used for fuselage, flight controls, landing gear, rotor hub and blades, gear box, and drive shaft. The data base behind these models includes small helicopters.

Table 1. Technology factors for all designs (net, including calibration factors).

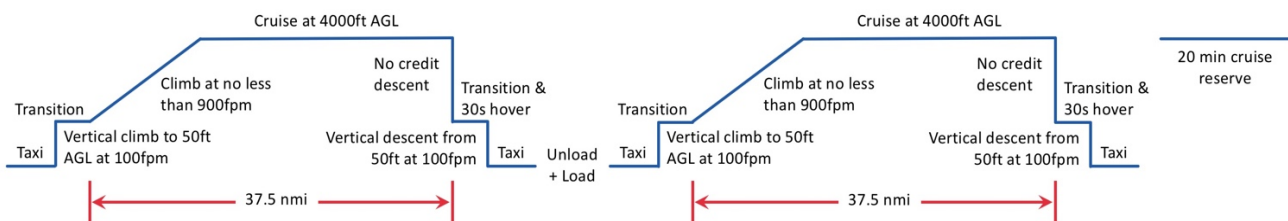|	
rotor flight control	
boosted controls	0.46
actuators	0.71
non-boosted controls	1.10
fuselage	
basic	0.76
crashworthiness	0.90
crash weight	6% basic
landing gear	
basic	1.00
crash weight	15% basic
rotor	
blade	0.92
hub	0.76
fuel tank	
tank	0.84
plumbing	0.66
drive system	
gear box	0.74
drive shaft	0.69
engine group	
cowling	0.50
pylon	0.85
support	1.10
accessories	0.82

Figure 7. UAM sizing mission profile (Ref. 3).

Traditional allocations are used for avionics equipment, for furnishings, and for environmental control. The technology factors reflect light-weight, rugged composite fuselage, light-weight composite rotor system, fuel efficient and light weight turboshaft engines, and weight efficient drive systems. Allocations for crashworthiness are included in the fuselage and landing gear weights. Table 1 gives the tech factors used in the designs. The flight controls are electric, hence there is no hydraulic system weight. Electrical system weight is 10 lb plus 10 lb/persion. Environmental system weight is 15 lb/person.

NOTAR Anti-Torque System

A NOTAR system consists of a variable pitch fan inside the tail boom, a circulation control boom for anti-torque when operating in the main rotor downwash, and a direct jet for yaw control (Ref. 46). The fan pressurizes the flow in the boom. A fraction of the flow (less than 10%) exits through slots in the tail boom, providing an anti-torque force on the boom through circulation control acting in the velocity from the main rotor wake. Most of the flow exits through a jet at the end of the boom, providing both anti-torque force and yaw control. A rotating sleeve controls the jet exit area and the direction of the jet. The pilot's pedals control both fan pitch and the orientation of the jet sleeve. In hover, the boom provides 55–70% of the anti-torque moment required. In cruise forward flight, the wake does not impinge on the boom, but the vertical tail provides 50–90% of the anti-torque moment required. In rearward and sideward flight, the direct jet provides most of the yaw control.

Reference 47 provides weight estimates for NOTAR systems. The body group weight increase is 69 lb for the MD500E (SDGW = 3000 lb), and is calculated to be 160 lb for the AH-64A (SDGW = 14600 lb). For the propulsion group, there is no tail rotor drive shaft and gear box; but there is a variable-pitch fan, gearbox, and drive shaft; for about 7% reduction in weight relative a tail rotor.

References 48–50 discuss noise of the NOTAR system, based on certification flight tests of the MD520N. In summary, they concluded: (a) takeoff noise depended on performance, the right side (away from jet) was quieter by 2.2 EPNdB; (b) approach noise was mainly from the rotor, 2.4 EPNdB quieter; (c) flyover noise was much quieter, by 6.5 EPNdB. The absence of the tail rotor was the dominant factor, although they did observe the first couple tones of fan noise. It is assumed here that the fan noise can be absorbed by proper boom design.

The NDARC model of the NOTAR system consists of a ducted fan at the location of the jet, oriented to produce the required anti-torque moment. The boom exit area is small compared to the jet exit area, so the boom mass flux is neglected. The boom momentum force is small compared to the jet force, and significantly less than the tail boom aerodynamic download due to the wake, so the boom momentum force is neglected. The boom anti-torque force is represented by simply an input fraction of the force produced by the fan. This fraction is reduced to zero when the boom is no longer immersed in the rotor wake. A body weight increment scaled with SDGW (based on Ref. 47) is used, and a 5% increase in fuselage wetted area.

Engines

Turboshaft technology is specified by weight/power and specific fuel consumption. The side-by-side turboshaft engine is based on the RR300 (TRL 9 since early 2000s) and Allison 250/T63-A-5 (1970s technology) engines, scaled as for the NDARC generic 500 hp engine model. The engine weight is 0.50 lb/hp, and the MCP SLS specific fuel consumption is 0.54 lb/hp-hr.

Quiet helicopter demonstration programs (OH-6A, Refs. 9–13; HH-43B, Refs. 8, 14; SH-3A, Ref. 15) included reducing the engine noise and testing sound-absorbing installations. Based on References 11–12, quieting the engine by 10 to 15 dB is possible, for a weight increase of around 40 lb per engine. For the present investigation, it is assumed that engine noise does not contribute to the observed sound, at a cost of 75 lb increase in engine installation weight.

Higher Harmonic Control

There have been numerous tests and demonstrations of higher harmonic control (HHC) and individual blade control (IBC): wind tunnel tests and flight tests, open and closed loop, 2/rev to 5/rev (summarized in Ref. 51). Typically 1 to 2° of blade pitch amplitude can influence the rotor behavior significantly, including a factor of 10 reduction of vibration at high speed (from 0.3–0.6 g, down to less than 0.05 g); 6 dB or more reduction of noise; or 5–7% reduction of power at high speed. Simultaneous reduction of noise and vibration has been achieved, using multiple harmonics of control. Rotor power often increases when the objective is just vibration or noise reduction. The pitch link loads, swashplate control loads, and blade torsion loads are increased for most cases. An HHC or IBC system adds weight to the aircraft and consumes power when active, but the goal is weight and power requirements that are less than for passive control (by vibration absorbers or blade design), with increased flexibility and effectiveness.

Table 2. Quiet Single Main Rotor helicopter characteristics.

main rotor tip speed (ft/sec)	700*	650	600	550	500	450	400
payload (lb)	1200	1200	1200	1200	1200	1200	1200
range (nm)	75	75	75	75	75	75	75
disk loading (lb/ft^2)	4	4	4	4	4	4	4
aircraft size							
DGW (lb)	3615	3660	3671	3739	3746	3912	4252
rotor radius (ft)	16.96	17.07	17.09	17.25	17.27	17.64	18.39
solidity	0.0411	0.0477	0.0559	0.0666	0.0805	0.0994	0.1258
number of blades	3	3	4	4	6	6	8
blade aspect ratio	22.8	19.6	22.3	18.7	23.2	18.8	19.8
power (hp)	2x215	2x217	2x218	2x221	2x216	2x231	2x280
sfc MCP SLS	0.576	0.575	0.575	0.575	0.575	0.574	0.570
drag D/q (ft^2)	5.02	5.06	5.08	5.14	5.14	5.29	5.61
D/q/(W/1000)$^{2/3}$	2.11	2.11	2.11	2.11	2.11	2.08	1.98
fuel tank capacity (lb)	170	168	167	168	172	186	221
weight							
WE (lb)	2235	2281	2294	2361	2364	2516	2821
structure	1011	1038	1047	1085	1092	1174	1319
rotor group	222	242	249	277	282	330	389
fuselage group	432	436	436	441	441	456	494
propulsion	575	586	595	612	615	664	794
drive system	164	173	182	195	203	231	297
systems	492	497	491	498	491	502	510
flight controls	91	94	86	89	78	82	78
performance							
cruise speed (knots)	102.05	103.63	103.04	103.91	106.94	105.41	97.43
V/V_{tip}	0.246	0.269	0.290	0.319	0.361	0.395	0.411
aircraft $L/D_e = WV/P$	5.07	5.21	5.30	5.39	5.36	5.06	4.50
rotor $L/D_e = LV/(P_i+P_o)$	9.47	9.91	9.60	9.18	8.48	7.45	6.42
aircraft figure of merit	0.610	0.613	0.613	0.616	0.630	0.636	0.642
rotor hover figure of meit	0.697	0.705	0.714	0.723	0.732	0.741	0.751
V_{br} (knots)	99.37	101.17	100.87	101.78	104.04	104.07	98.07
V_y (knots)	84.58	87.12	89.01	88.92	82.11	76.65	69.35
V_H (knots)	110.58	111.84	112.96	114.87	117.15	117.85	112.64
noise conditions							
WMTO (lb)	3667	3714	3725	3795	3802	4059	4761
altitude (ft)	0	0	0	0	0	0	0
temperature (ºF)	77	77	77	77	77	77	77
takeoff, V_y (knots)	85.73	88.19	90.00	89.80	82.95	77.41	70.02
takeoff, ROC (ft/min)	1415	1387	1344	1273	1188	1093	982
takeoff, climb angle (deg)	9.4	8.9	8.5	8.0	8.1	8.0	8.0
flyover, V (knots)	99.52	100.66	101.66	103.38	105.43	106.06	101.38
approach, V_y (knots)	85.05	87.60	89.50	89.41	82.56	77.07	69.73
approach, ROC (ft/min)	-900	-927	-947	-946	-874	-816	-738
approach, descent angle (deg)	6	6	6	6	6	6	6

* Baseline aircraft. All designs have NOTAR anti-torque system and quieted turboshaft engine.

QSMR DESIGNS

The single main rotor helicopter designs for tip speeds from 700 ft/sec down to 400 ft/sec are summarized in Table 2. The rotor has an articulated hub, with the flap hinge at 0.045R. The blades use a modern, 11% thick airfoil, with –12 deg twist and 60% tapered tip (from 0.94R). The root cutout is 0.15R. Figures 8 and 9 present the variation of the basic aircraft parameters with design tip speed. The design disk loading and blade loading are $T/A = 4$ lb/ft^2 and $C_W/\sigma = 0.10$, so blade area and solidity increase as the tip speed is reduced. The blade number is increased with solidity, to keep the blade aspect ratio high. A consequence of the increased blade area is increased weight and power, which becomes significant at 450 ft/sec tip speed and below. Figure 10 illustrates the rotor geometry for different design tip speeds. For the baseline high tip speed (700 ft/sec) and low disk loading, the solidity is low and the blade aspect ratio is high (22.8). As the tip speed decreased and the solidity increased, the number of blades was increased to keep the aspect ratio high. Low aspect-ratio blades are inefficient aerodynamically, acoustically (thick sections), and structurally (control system weight).
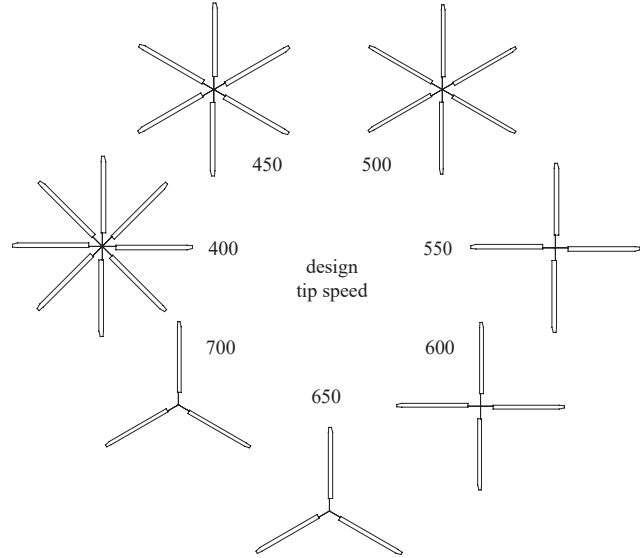

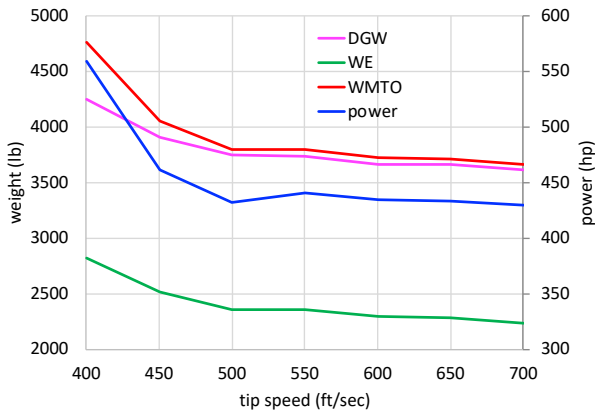Figure 10. Rotor geometry for variation in design tip speed (ft/sec).

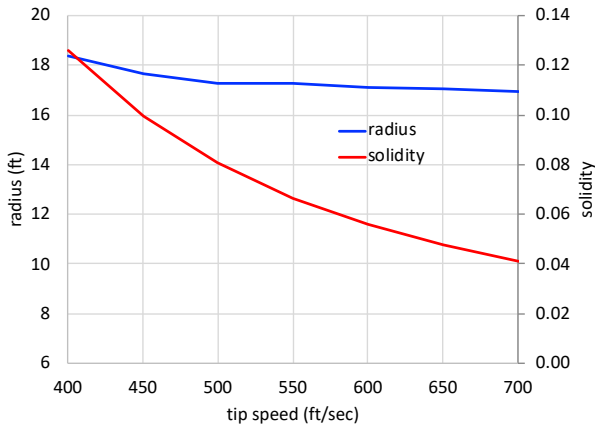Figure 8. Aircraft weight and power variation with design tip speed.

Figure 9. Rotor radius and solidity variation with design tip speed.

IMPACT OF DESIGN FOR LOW NOISE

The noise was calculated for each of the rotorcraft designs, in terms of the EPNL at the takeoff, flyover, and approach certification conditions. Table 2 gives the operating conditions (weight, atmosphere, speed, and rate of climb or descent) for each of the designs. The duration of each noise event (PNLT with 10 dB of the peak, contributing to EPNL) is about 11 sec at these flight speeds. Generally, the noise is largest for the centerline microphone, and smallest for the microphone on the retreating side of the disk (port side). Thickness noise does not contribute significantly to the OASPL, even for 700 ft/sec tip speed. The loading noise is dominant for approach and flyover, while the broadband noise is important for takeoff. In all three conditions, the broadband noise is dominant at high frequencies (above 1000 Hz for approach), but does not contribute to PNLT when the loading noise is significant at lower frequencies.

This investigation uses the certification metric to assess the impact of design parameters on the helicopter noise. With the assumption of compact loading in the noise calculation, a comparison with the certification requirement is not appropriate, rather the noise is compared with that of the baseline aircraft with typical (high) tip speed (700 ft/sec), conventional blade planform, and no higher-harmonic control. All aircraft, including the baseline, have the NOTAR anti-torque system and quieted engines. While the assumption of compact loading must affect the accuracy of the noise calculations, it is expected the trends are good, even quantitatively. All EPNL results are shown here (Figures 11–13) relative the loudest value: the baseline aircraft approach noise.
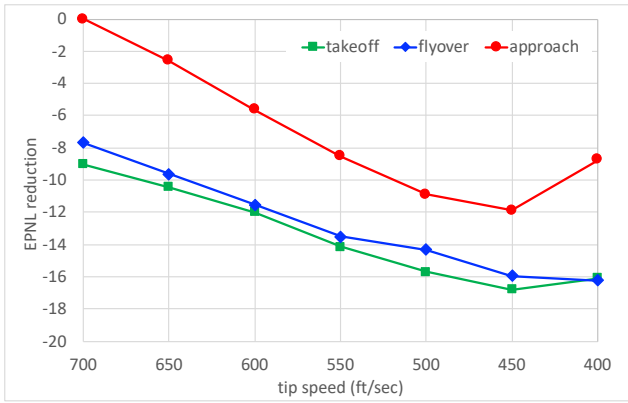
Figure 11. Impact of design rotor tip speed on takeoff, flyover, and approach noise.
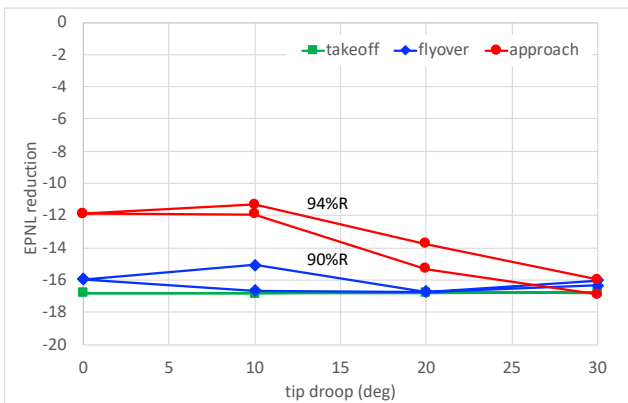

Figure 12. Reduction in noise with droop of blade tip, beginning at 94%R and 90%R (tip speed 450 ft/sec).
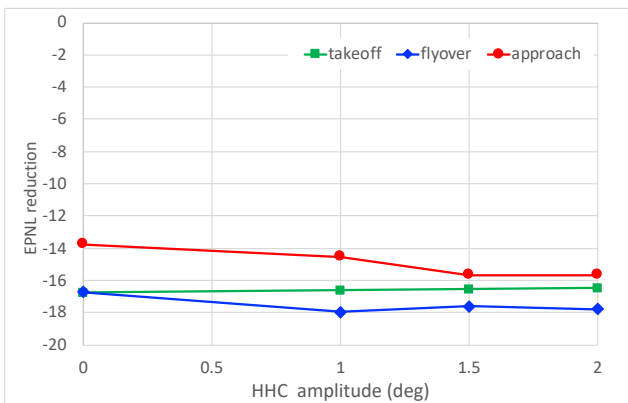

Figure 13. Reduction in noise with amplitude of $\sin(3\psi)$ individual blade control (tip speed 450 ft/sec, 20° tip droop at 94%R)

Figure 11 shows the impact of design rotor tip speed on the takeoff, flyover, and approach noise. As usual, noise levels are highest in approach, because of blade-vortex interaction. Relative a conventional tip speed of 700 ft/sec, designing for a tip speed of 450 ft/sec reduces the EPNL by 12 dB.

The aircraft gets larger as the tip speed is reduced, which directly affects the noise. The maximum takeoff weight increases from 3667 lb at 700 ft/sec tip speed, to 4059 lb at 450 ft/sec. The weight empty is about the same as the turboshaft-powered side-by-side helicopter of Ref. 4. Designed to 400 ft/sec tip speed, the QSMR maximum takeoff weight is 4761 lb, and the noise is larger than for 450 ft/sec.

Drooping the blade tip can further reduce the approach noise (Figure 12), by moving the tip vortices away from the following blades and hence reducing blade-vortex interaction noise. Higher harmonic control or individual blade control can reduce approach noise as well, although not by as much as would be expected for a high tip-speed design. Rotating frame blade root pitch control of $\sin(3\psi)$ can reduce the approach noise by 2 dB in this case, for a tip speed of 450 ft/sec, and 20° tip droop at 94%R.

CONCLUDING REMARKS

A single main-rotor helicopter designed specifically for low-noise air taxi operations has been described. Several design parameters were explored to reduce the noise, including rotor tip speed, blade geometry, and higher-harmonic control. The metric was the reduction of the noise for the helicopter certification conditions (takeoff, flyover, and approach), relative a baseline aircraft with typical (high) tip speed, conventional blade planform, and no higher-harmonic control. Designing the aircraft with a tip speed to 450 ft/sec reduced the approach EPNL by 12 dB relative a design for 700 ft/sec, with only a small increase in aircraft weight. Takeoff and flyover noise were reduced by 8 dB. Droop of the blade tip and use of individual blade control further reduced the approach noise further, for a total reduction of 16 dB.

The investigation will continue with more complete noise calculations using NASA's ANOPP2 software, based on CFD calculations of the rotor blade airloads, with the objective of confirming the impact of design choices and making quantitative predictions of the aircraft noise relative helicopter certification requirements.

REFERENCES

1) Silva, C.; Johnson, W.; and Solis, E. "Multidisciplinary Conceptual Design for Reduced-Emission Rotorcraft." American Helicopter Society Technical Conference on Aeromechanics Design for Transformative Vertical Flight, San Francisco, CA, January 2018.

2) Johnson, W.; Silva, C.; and Solis, E. "Concept Vehicles for VTOL Air Taxi Operations." American Helicopter Society Technical Conference on Aeromechanics Design for Transformative Vertical Flight, San Francisco, CA, January 2018.

3) Patterson, M.D.; Antcliff, K.R.; and Kohlman, L.W. "A Proposed Approach to Studying Urban Air Mobility Missions Including an Initial Exploration of Mission Requirements." American Helicopter Society 74th Annual Forum, Phoenix, AZ, May 2018.

4) Silva, C.; Johnson, W.; Antcliff, K.R.; and Patterson, M.D. "VTOL Urban Air Mobility Concept Vehicles for Technology Development." AIAA Paper No. 2018-3847, June 2018.

5) Cox, C.R. "Helicopter Noise Reduction and Its Effects on Operations." Journal of the American Helicopter Society, *15*:1 (January 1970).

6) Faulkner, H. "The Cost of Noise Reduction in Helicopters." MIT FTL Report R71-5, November 1971.

7) Simpson, R.W.; Faulkner, H.B.; and Hays, A.P. "A Systems Study of Noise Requirements on the Design of V/STOL Aircraft." U.S. Army Research Office, Helicopter Noise Symposium, Durham, NC, September 1971.

8) Hilton, D.A.; Henderson, H.R.; and Pegg, R.J. "Ground Noise Measurements During Flyover, Hover, Landing, and Take-Off Operations of a Standard and a Modified HH-43B Helicopter." NASA TM X-2226, February 1971

9) Hirsh, N.B., and Ferris, H.W. "Design Requirements for a Quiet Helicopter." American Helicopter Society 28th Annual National Forum, Washington, D.C., May 1972.

10) Barlow, W.H.; McCluskey, W.C.; and Ferris, H.W. "OH-6A Phase II Quiet Helicopter Program." USAAMRDL TR 72-29, September 1972.

11) Robinson, F. "Component Noise Variables of a Light Observation Helicopter." NASA CR 114761, 1973.

12) Wagner, R.A. "Noise Levels of Operational Helicopters of the OH-6 Type Designed to Meet the LOH Mission." NASA CR 114760, 1973.

13) Henderson, H.R.; Pegg, R.J.; and Hilton, D.A. "Results of the Noise Measurement Program on a Standard and Modified OH-6A Helicopter." NASA TN D-7216, September 1973.

14) Bowes, M.A. "Test and Evaluation of a Quiet Helicopter Configuration HH-43B." Journal of the Acoustical Society of America, *54*:5 (November 1973).

15) Pegg, R.J.; Henderson, H.R.; and Hilton, D.A. "Results of the Flight Noise Measurement Program Using a Standard and Modified SH-3A Helicopter." NASA TN D-7330, December 1973.

16) Faulkner, H.B. "The Cost of Noise Reduction in Intercity Commercial Helicopters." Journal of Aircraft, *11*:2 (February 1974).

17) Stuelpnagel, T.R. "The Coming Era of the Quiet Helicopter." The Aeronautical Journal, *109*:1090 (December 1975).

18) Bowes, M.A. "Helicopter Noise Reduction Design Trade-Off Study." Federal Aviation Administration, Report FAA AEQ-77-4, January 1977.

19) Spencer, R.H. "A Study of the Economic Impact of Noise Limits on New Design and Current Production Helicopters." American Helicopter Society 36th Annual Forum, Washington, D.C., May 1980.

20) Leverton, J.W. "Reduction of Helicopter Noise by Use of a Quiet Tail Rotor." Vertica, *6*:1 (1982).

21) Shenoy, K.R.; Moffitt, R.C.; Yoerkie, C.A.; and Childress, O., Jr. "Development and Validation of "Quiet Tail Rotor" Technology." American Helicopter Society International Technical Specialists Meeting, Rotorcraft Aeroacoustics and Rotor Fluid Dynamics, Philadelphia, PA, October 1991.

22) Kearsey, P.R. "Helicopter Noise Certification." Royal Aeronautical Society Conference on the Quiet Helicopter, London, UK, March 1992.

23) Simson, J., and Freeborn, P. "Helicopter Noise — Public Perspective." Royal Aeronautical Society Conference on the Quiet Helicopter, London, UK, March 1992.

24) Lowson, M.V. "Progress Towards Quieter Civil Helicopters." The Aeronautical Journal, *96*:956 (June/July 1992).

25) Perry, F.J., and Pike, A.C. "Helicopter Aeroacoustics and the Impact of Noise Regulations on Design." Royal Aeronautical Society Conference on the Quiet Helicopter, London, UK, March 1992.

26) Delrieux, Y.; Prieur, J.; and Declerck, D. "Aeroacoustic Prediction Tools for Quiet Rotor Design and Optimization at ONERA." American Helicopter Society Aeromechanics Specialists Conference, San Francisco, CA, January 1994.

27) Leverton, J.W. "The Potential for Quiet Rotorcraft." CEAS/AIAA Paper No. 95-005, June 1995.

28) Niesl, G., and Arnaud, G. "Low Noise Design of the EC 135 Helicopter." American Helicopter Society 52nd Annual Forum, Washington, D.C., June 1996.

29) Allongue, M.; Marze, H.J.; and Potdevin, F. "The Quiet Helicopter — From Research to Reality." American Helicopter Society 55th Annual Forum, Montreal, Canada, May 1999.

30) Bebesel, M.; D'Alascio, A.; Schneider, S.; Guenther, S.; Vogel, F.; Wehle, C.; and Schimke, D. "Bluecopter Demonstrator — An Approach to Eco-Efficient Helicopter Design." Forty-First European Rotorcraft Forum, Munich, Germany, September 2015.

31) Schneider, S.; Heger, R.; and Konstanzer, P. "BLUECOPTER^TM Demonstrator: The State-of-the-Art in Low Noise Design." Forty-Second European Rotorcraft Forum, Lille, France, September 2016.

32) Stevens, J.; Smith, C.; Thevenot, L.; d'Ippolito, R.; Gires, E.; Castillo Pardo, A.; and Pachidis, V. "CleanSky Green Rotorcraft New Technologies — Maximizing Noise and Emissions Benefits." Forty-Second European Rotorcraft Forum, Lille, France, September 2016.

33) Guntzer, F.; Gareton, V.; Pinacho, J.-P.; and Caillet, J. "Low Noise Design and Acoustic Testing of the Airbus Helicopter H160-B." Forty-Fifth European Rotorcraft Forum, Warsaw, Poland, September 2019.

34) Schlegel, R.; King, R.; and Mull, H. "Helicopter Rotor Noise Generation and Propagation." USAAVLABS TR 66-4, October 1966.

35) Johnson, W. "NDARC. NASA Design and Analysis of Rotorcraft." NASA TP 2015-218751, April 2015.

36) Johnson, W., "Technology Drivers in the Development of CAMRAD II," American Helicopter Society Aeromechanics Specialist Meeting, San Francisco, California, January 1994.

37) Johnson, W. "Rotorcraft Aeromechanics Applications of a Comprehensive Analysis." HeliJapan 1998: AHS International Meeting on Rotorcraft Technology and Disaster Relief, Gifu, Japan, April 1998.

38) Boyd, D.D., Jr.; Greenwood, E.; Watts, M.E.; and Lopes, L.V. "Examination of a Rotorcraft Noise Prediction Method and Comparison to Flight Test Data." NASA TM 2017-219370, January 2017.

39) Ffowcs Williams, J.E., and Hawkings, D. "Sound Generation by Turbulence and Surfaces in Arbitrary Motion.'" Philosophical Transactions of the Royal Society of London, 264A:1151 (May 1969).

40) Farassat, F. "Theory of Noise Generation From Moving Bodies With an Application to Helicopter Rotors." NASA TR R-451, December 1975.

41) Farassat, F. "Linear Acoustic Formulas for Calculation of Rotating Blade Noise." AIAA Journal, 9:9 (September 1981).

42) Pegg, R.J. "A Summary and Evaluation of Semi-Empirical Methods for the Prediction of Helicopter Rotor Noise." NASA TM 80200, December 1979.

43) Brooks, T.F.; Pope, D.S.; and Marcolini, M.A. "Airfoil Self-Noise and Prediction." NASA RP 1218, July 1989.

44) Weir, D.S.; Jumper, S.J.; Burley, C.L.; and Golub, R.A. "Aircraft Noise Prediction Program Theoretical Manual. Rotorcraft System Noise Prediction System (ROTONET). Rotor Broadband Noise (RBN) Module." NASA TM 83199, Part 4, April 1995.

45) United States Government, "Part 36 — Noise Standards, Aircraft Type and Airworthiness Certification." Code of Federal Regulations, Title 14, Aeronautics and Space.

46) Sampatacos, E.P.; Hanvey, S.A.; Harrison, J.M.; King, R.J.; Logan, A.H.; and Morger, K.M. "Design, Development, and Flight Test of the No Tail Rotor (NOTAR) Helicopter" USAAVRADCOM TR 82-D-41, May 1983.

47) Vega, E. "Advanced Technology Impacts on Rotorcraft Weight." Journal of the American Helicopter Society, 31:4 (October 1986).

48) Currier, J.M.; Hardesty, M.; and O'Connell, J.M. "NOTAR System — A Quiet Character." American Helicopter Society International Technical Specialists Meeting, Rotorcraft Aeroacoustics and Rotor Fluid Dynamics, Philadelphia, PA, October 1991.

49) Hardesty, M.; Mejia, K.; Currier, J.; and Hudson, B. "Noise Certification Flight Tests of MDHC Light Helicopters." American Helicopter Society and Royal Aeronautical Society International Technical Specialists Meeting: Rotorcraft Acoustics and Rotor Fluid Dynamics, Valley Forge, PA, October 1991.

50) JanakiRam, R.D., and Currier, J.M. "Noise Characteristics of Helicopters With the NOTAR Anti-Torque System." Royal Aeronautical Society Conference on the Quiet Helicopter, London, UK, March 1992.

51) Johnson, W. Rotorcraft Aeromechanics. New York: Cambridge University Press, 2013.

NOMENCLATURE

DGW	design gross weight
DL	disk loading, GW divided by rotor disk area
EPNL	effective perceived noise level
FM	aircraft or rotor figure of merit
GW	gross weight (WO+payload+fuel)
IRP	intermediate rated power (typically 30 min)

ISA	international standard atmosphere	D/q	drag divided by dynamic pressure
MCP	maximum continuous power	L	rotor lift
MRP	maximum rated power (typically 10 min)	L/D_e	aircraft effective lift-to-drag ratio, WV/P
NOTAR	NO TAil Rotor anti-torque system	L/D_e	rotor effective lift-to-drag ratio, $LV/(P_o+P_i)$
OASPL	overall sound pressure level	P	power
OGE	out-of-ground-effect	P_o	profile power
PNL	perceived noise level	P_i	induced power
QSMR	quiet single-main-rotor helicopter	R	rotor blade radius
ROC	rate of climb	T	rotor thrust
SDGW	structural design gross weight	V	speed
sfc	specific fuel consumption	V_{be}	best endurance speed (max 1/fuelflow)
SLS	sea-level standard	V_{br}	best range speed (99% max V/fuelflow)
VTOL	vertical take-off and landing	V_{cruise}	cruise speed
WE	aircraft empty weight	V_H	maximum speed (100% MCP)
WO	operating weight empty	V_{max}	maximum speed (90% MCP)
WMTO	maximum takeoff weight	V_{tip}	rotor tip speed
		V_y	best reate of climb speed (100% MRP)
A	rotor disk area, πR^2	W	weight
A_{blade}	total blade area	ρ	air density
C_T	rotor thrust coefficient, $T/\rho A V_{tip}^2$	σ	rotor solidity, A_{blade}/A
C_T/σ	blade loading, $T/\rho A_{blade} V_{tip}^2$		
C_W	aircraft weight coefficient, $W/\rho A V_{tip}^2$		